Engineering 21 (2023) 101–114

Contents lists available at ScienceDirect

Engineering

journal homepage: www.elsevier.com/locate/eng

Research
Frontier Research on Carbon Neutrality—Review

CO_2 High-Temperature Electrolysis Technology Toward Carbon Neutralization in the Chemical Industry

Yifeng Li [a], Longgui Zhang [a], Bo Yu [b], Jianxin Zhu [c], Changjiang Wu [a,*]

[a] SINOPEC (Beijing) Research Institute of Chemical Industry Co., Ltd., Beijing 100013, China
[b] Institute of Nuclear and New Energy Technology, Tsinghua University, Beijing 100084, China
[c] Research Center for Eco-Environmental Sciences, Chinese Academy of Sciences, Beijing 100085, China

ARTICLE INFO

Article history:
Received 3 September 2021
Revised 9 November 2021
Accepted 28 February 2022
Available online 1 September 2022

Keywords:
Solid oxide electrolysis cell
Carbon dioxide
Carbon neutralization
Nickel
Perovskite
Scale-up

ABSTRACT

The chemical industry is a major carbon emitter in China and must be focused on for China to achieve its goal of carbon neutralization. Carbon dioxide (CO_2) high-temperature electrolysis based on solid oxide electrolysis cells (SOECs) is an important technology to achieve China's carbon emission reduction, peak carbon emission, and carbon neutralization goals. Moreover, this technology can realize the recycling utilization of CO_2 and thereby contribute to considerable environmental benefits and potential economic benefits. Thus far, a great deal of progress has been made in CO_2 high-temperature electrolysis technology at the laboratory stage and pilot stage, although the large-scale industrial application of this technology still requires further development. This review focuses on recent progress in state-of-the-art cell materials for high-temperature CO_2 electrolysis, discusses the future research directions of SOEC technologies, and proposes possible SOEC-coupled chemical industry carbon neutralization solutions.

1. Introduction

The chemical industry is a major carbon emitter in China and must be focused on for China to achieve its goal of carbon neutralization. In the past ten years, carbon dioxide (CO_2) emissions from the coal chemistry and petrochemical industries around the world have increased by more than 50 times (from 0.91 billion tonnes per year to 49 billion tonnes per year), and the contradiction between China's aims of industrial development and environmental protection is becoming increasingly serious [1,2]. Recently, China stated its goal of achieving peak carbon emissions by 2030 and carbon neutralization by 2060. Carbon neutralization requires the carbon sink (i.e., the total amount of CO_2 that is absorbed by plants and captured by humans) to able to completely offset carbon emissions. However, the current carbon sink in China is only about 1.5 billion tonnes per year, which is significantly less than the carbon emissions of the chemical industry [2]. Obviously, a huge gap needs to be crossed to achieve the goal of carbon neutralization.

Taking the coal chemical industry as an example, in modern coal chemical production, only 1/5–1/3 of the carbon in raw coal goes into products; the rest becomes a source of huge amounts of carbon emissions [2]. Furthermore, half of the energy consumption is directly discarded in various forms and eventually becomes ambient thermal pollution. Given these problems, in addition to significantly reducing the proportion of traditional fossil energy (e.g., coal, oil) in the energy structure, the efficient recycling utilization of CO_2 and waste heat holds great importance [3]. Recently, high-temperature electrolysis technology based on solid oxide electrolysis cells (SOECs) has attracted increasing attention worldwide [1,4]. In combination with renewable energy, such as the rich wind power or photovoltaic energy in northwest China, SOECs operating at elevated temperatures can not only make full use of industrial waste heat but also convert CO_2 into hydrocarbon fuel or high-value-added chemical products via electrochemical reactions, thereby simultaneously realizing the large-scale storage of renewable energy and the efficient utilization of CO_2 (Fig. 1) [4–6]. More importantly, compared with other electrochemical techniques at lower temperature conversions ($\leq$200 °C), such as transition metal electrodes in liquid electrolytes, SOECs operating at high temperatures of 800–1000 °C possess many unique advantages, including low impedance, low power consumption, high electrolysis efficiency, and less dependency on noble metal electrode catalysts [2]. Moreover, SOECs have the potential to

* Corresponding author.
E-mail address: wuchangjiang.bjhy@sinopec.com (C. Wu).

https://doi.org/10.1016/j.eng.2022.02.016

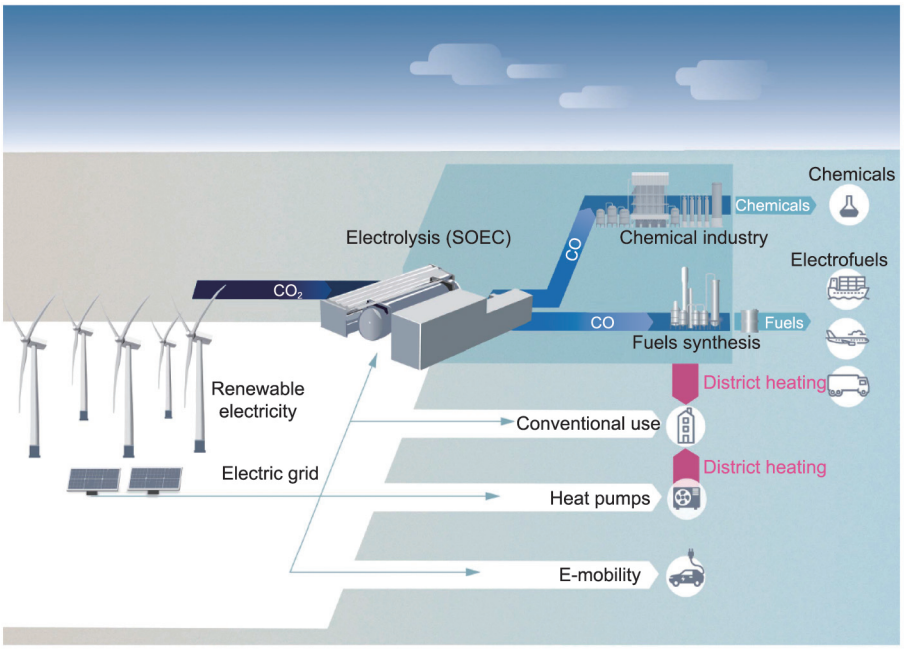

Fig. 1. The high-efficiency conversion and utilization of CO_2 in chemical processes based on high-temperature electrolysis. Reproduced from Ref. [4] with permission.

operate stably even at relatively high current densities. As a comparison, the operating current density of alkaline electrolysis cells (AECs) is typically lower than 0.5 A·cm^{-2}, while state-of-the-art SOECs can operate at a high current density of above 1.0 A·cm^{-2} with low polarization loss and ignorable performance degeneration [4,7]. This implies that an SOEC stack can be designed to be much smaller than an AEC stack with the same electrolysis capacity. Therefore, SOECs can potentially be used to achieve modular flexible design for application in certain specific scenarios [2,7].

2. The SOEC for CO_2 conversion

There are two main CO_2 conversion approaches using SOECs at high temperature: pure CO_2 electrolysis to CO and O_2; and CO_2 electrolysis in the presence of other substances (H_2O, CH_4, etc.), which is referred to as co-electrolysis and includes CO_2/H_2O and CO_2/CH_4 co-electrolysis [1]. This review article discusses both pure CO_2 electrolysis and co-electrolysis in regard to CO_2 high-temperature electrochemical conversion. The structure of a basic unit for CO_2 conversion using SOEC is illustrated in Fig. 2 (in the case of pure CO_2 electrolysis). This basic unit typically consists of a cathode, an electrolyte, and an anode. During the CO_2 electrolysis (or co-electrolysis) process, CO_2 (or CO_2/H_2O) molecules are reduced at the cathode/electrolyte interface to generate gaseous CO (or CO/H_2) and O^{2-}. These gases subsequently pass through the porous electrode with the assistance of a carrier gas; the generated O^{2-} migrates through the dense electrolyte layer at elevated temperatures, and is subsequently discharged at the electrolyte/anode interface to generate gaseous O_2 [8–12]. The main reactions include the following:

Cathode:

$$CO_2 + 2e^- \rightarrow CO + O^{2-} \quad (1)$$

Anode:

$$O^{2-} - 2e^- \rightarrow \frac{1}{2}O_2 \quad (2)$$

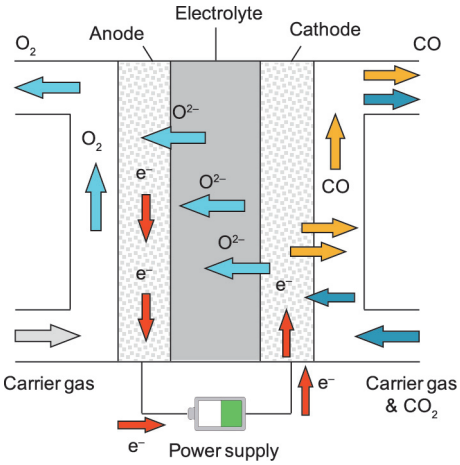

Fig. 2. Schematic diagram of the basic structure of an SOEC for CO_2 conversion.

Total reaction:

$$CO_2 \rightarrow CO + \frac{1}{2}O_2 \quad (3)$$

The co-electrolysis of CO_2/H_2O can not only realize the efficient conversion of electrical energy into chemical energy (H_2 + CO, known as syngas) but also solve the problem of the recycling utilization of CO_2; thus, this technology has attracted a considerable amount of attention [2,12]. CO_2/H_2O co-electrolysis is much more complicated than steam electrolysis due to the existence of the reverse water gas shift (RWGS) reaction, in which H_2O is reduced into H_2 in the forward electrolysis reaction, and CO_2 is subsequently reduced by H_2 [2,13]:

$$H_2 + CO_2 \rightarrow H_2O + CO \quad (4)$$

According to the existing literature, the Gibbs free energy change (ΔG) of the RWGS reaction is positive at relatively low temperatures but drops to 0 when the temperature is increased

to approximately 800 °C [2]. This finding suggests that RWGS can be thermodynamically spontaneous under high-temperature co-electrolysis conditions (e.g., in the temperature range of 800–1000 °C) and that increasing the temperature can further promote the conversion of CO_2. The syngas produced by co-electrolysis can be further utilized in various chemical synthesis scenarios to produce a series of high-value-added products, such as methane, methanol, or ethylene [1,2,14].

Compared with co-electrolysis, pure CO_2 electrolysis is less dependent on water resources—a characteristic that is of great importance in achieving carbon neutralization—although it possesses a higher technical threshold and presents more challenges at present stage [2,12]. With recent developments in the fundamental theory of electrochemistry and progress in related technologies, CO_2 electrolysis is expected to become an emerging industrial technology [1,2]. In the National Aeronautics and Space Administration (NASA) Mars Exploration Program, SOECs were utilized to electrolyze the rich CO_2 in the Martian atmosphere to fabricate oxygen propellant for space rovers [15].

Despite the broad application prospects of CO_2 electrolysis or co-electrolysis, it should be noted that the molecular structure of CO_2 is fundamentally more stable than that of H_2O; thus, it is more difficult to cause CO_2 electrolysis or co-electrolysis, in comparison with steam electrolysis. Therefore, novel SOEC component materials with relatively high electrochemical activity and operation stability should be developed to realize steady CO_2 electrolysis or co-electrolysis [16]. The next sections introduce the latest research progress in SOEC cathodes, electrolytes, anodes, and other component materials that are applicable for CO_2 electrolysis or co-electrolysis. Furthermore, the fundamental mechanism of the high-temperature electrochemical interfacial reactions in SOECs is discussed in detail to provide guidance for the rational design and optimization of high-performance cell components, as well as the design and integration of industrial-scale SOEC stacks and modules.

3. Core components of an SOEC

3.1. Cathode materials

During the CO_2 electrolysis process, CO_2 molecules are discharged onto the SOEC cathode, a carbon reduction reaction occurs, and oxygen ions are generated (Eq. (1)). This reaction involves the fracture of two π_3^4 bonds in the CO_2 molecule and requires a relatively high activation energy. Hence, the fracture of the π_3^4 bonds is regarded as the rate-determining step in the whole CO_2 electrolysis process. In order to reduce the activation energy and accelerate the reaction kinetics, the following characteristics are desirable for cathode materials: ① considerable electronic conductivity; ② considerable ionic conductivity; ③ the capability of chemical adsorption with CO_2 molecules; and ④ coking resistance, in order to prevent coke from being generated and accumulating via the excessive reduction of CO_2 during the electrolysis process.

3.1.1. Metal-containing cathodes

A series of metal–ceramic composite materials, such as the commonly used nickel–yttria-stabilized zirconia (Ni–YSZ), are currently the most extensively researched SOEC cathode materials. The classic fabrication method for a Ni–YSZ cathode involves co-combusting a mixture of nickel oxide (NiO), yttria-stabilized zirconia (YSZ), and pore formers (e.g., starch, poly(methyl methacrylate) (PMMA)) under oxidizing conditions, and then further reducing the mixture under a hydrogen (H_2) atmosphere to obtain the target product [2]. In a Ni–YSZ composite electrode, metallic nickel (Ni) possesses good electronic conductivity and can provide active sites for CO_2 chemical adsorption and electrochemical reduction. Sintered YSZ ceramic has good ionic conductivity and high mechanical strength, and thus plays a critical role in supporting the cathode. The pore former leads to the formation of a large number of pores in the electrode bulk phase after sintering, which can provide numerous channels for the diffusion and release of gaseous productions, such as H_2 and CO.

Thus far, the electrochemical performance and durability of Ni–YSZ electrodes have been widely investigated in CO_2 electrolysis and CO_2/H_2O co-electrolysis at the laboratory scale. In 2007, the Risø National Laboratory in Denmark reported that their Ni–YSZ|YSZ|LSM–YSZ (LSM stands for $La_{1-x}Sr_xMnO_{3-\delta}$) stacks achieved stable CO_2 electrolysis in a mixed atmosphere of 70% CO_2 + 30% CO at 950 °C [9]. The operating current density reached 1.5 A·cm^{-2} under a 1.29 V voltage, and the CO output reached 33 L·h^{-1}. Another case in point was conducted by the Risø National Laboratory and Haldor Topsøe A/S, in which the researchers put 12 cm × 12 cm 10-cell SOEC stacks (Ni–YSZ|YSZ|LSM–YSZ) in a mixed atmosphere of 45% H_2O + 45% CO_2 + 10% H_2 [17]. At 850 °C, stable electrolysis was achieved for 800 and 400 h under a current density of 0.50 and 0.75 A·cm^{-2}, respectively, and no performance degradation was detected during operation. Despite these results, several studies have still indicated that Ni–YSZ cathodes may undergo a degradation process at high current densities or during long-term operation. For example, researchers from the Jülich Research Center investigated the long-term performance of Ni–YSZ|YSZ|LSCF (LSCF stands for lanthanum strontium cobalt ferrite) stacks in an $H_2O/CO_2/H_2$ mixed atmosphere and found that the performance degradation rate was approximate 2%–4% per 1000 h when the current density was in the range of 0.300 to 0.875 A·cm^{-2}; moreover, the performance degradation rate increased to as high as about 6% per 1000 h when the electrolysis current density was elevated to above 0.875 A·cm^{-2} [18].

The degradation mechanism of Ni–YSZ cathodes during CO_2 electrolysis operation has also been extensively studied. Using impedance spectroscopy, Hauch et al. [19] investigated a Ni–YSZ|YSZ|LSM–YSZ stack and demonstrated that degradation of the electrolysis cell performance was significantly related to the increase in the polarization impedance of the Ni–YSZ cathode. In particular, they found that, under high temperature (e.g., 950 °C) and relatively high current density (e.g., 2 A·cm^{-2}), Ni migration and agglomeration were more likely to occur, significantly influencing the composition of the cathode/electrolyte interface, such as the formation of a dense Ni layer or a dense YSZ layer at the interfacial region, and significantly increasing the impedance of the cathodes. In another study, Skafte et al. [5] used *in situ* X-ray photoelectron spectroscopy (XPS) to investigate the degradation behavior of Ni–YSZ thin-film electrodes in a CO/CO_2 atmosphere. They noticed obvious C—C sp^2 and C—C sp^3 signals on the electrode surface when the overpotential was increased to 150 mV at 750 °C, which were recognized to be from deposited coke, as demonstrated by scanning electron microscopy (SEM) (Fig. 3) [5]. Argyle and Bartholomew [20] proposed that the deposited coke may originate from the disproportionation reaction of CO on the surface of metallic Ni.

To improve the electrocatalytic activity and stability of the Ni–YSZ cathode during CO_2 electrolysis at high temperature and high current density, researchers have developed various optimizing and modifying approaches, including surface modification by CeO_2-based oxides [5,21–24]. For example, in the *in situ* XPS investigation carried out by Skafte et al. [5], it was found that, after replacing the YSZ component in the cathode with $Sm_{0.2}Ce_{0.8}O_{1.9-\delta}$ (SDC) nanoparticles, carbon deposition did not occur until the extrinsic overpotential increased to about 300 mV, suggesting significantly enhanced surface coke resistance of the cathode in a CO/CO_2 atmosphere (Fig. 3(b)).

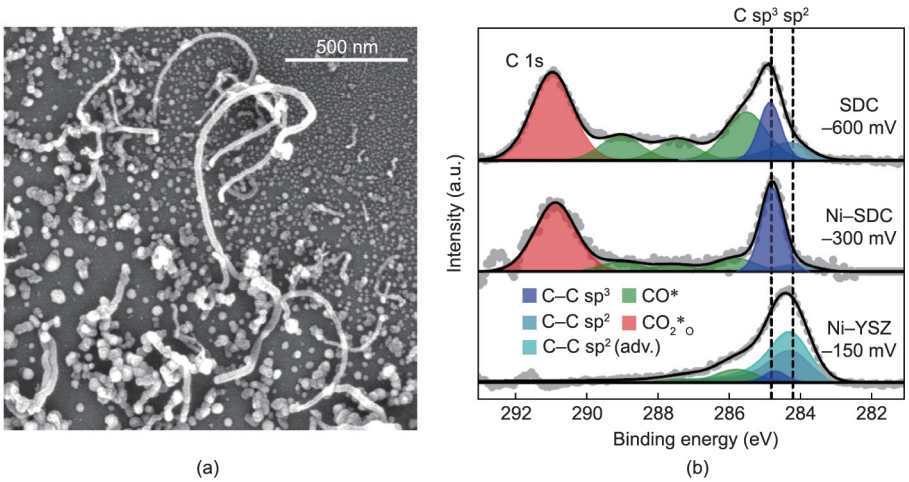

Fig. 3. (a) SEM image of the Ni–YSZ surface after carbon deposition; (b) XPS peaks for three respective electrodes (Ni–YSZ, Ni–SDC, and SDC) at the overpotential when the cathodes started to deposit carbon in a CO/CO_2 atmosphere (a.u.: absorbance unit). Reproduced from Ref. [5] with permission.

Extensive mechanism research has focused on possible reaction pathways for high-temperature CO_2 reduction in SOEC systems. The results not only reveal the origin of carbon deposition but also provide guidance for the rational optimization of existing Ni–YSZ-based cathode materials [5,20]. As illustrated in Fig. 4(a), it has been accepted that the CO_2 reduction reaction on a Ni/YSZ surface involves the following fundamental steps: ① the absorption and activation of CO_2 on the metallic Ni (surface + CO_2 (g) → CO_2^*); ② the breaking of the C═O double bond with the assistance of electron injection ($CO_2^* + 2e^- \rightarrow CO^* + \mu_O$); and ③ the desorption of CO ($CO^* \leftrightarrow CO$ (g)) [5]. The efficient utilization of CO_2 requires catalysts that can activate the first C═O double bond of CO_2 while suppressing complete deoxidation and avoiding overreduction ($CO^* + 2e^- \rightarrow C^* + \mu_O$) [5]. Unfortunately, theoretical simulation results suggest that coke generation on the Ni surface under the operating conditions is thermodynamically spontaneous. Under actual operation conditions, the coke-deposition phenomenon is widely observed, leading to the blocking of active sites on the cathode surface [5,17–19]. This is one of the most important degeneration issues of Ni–YSZ cathodes during the CO_2 electrolysis process.

As emerging candidates for SOEC cathode material, CeO_2-related oxides can significantly enhance the long-term stability of the cathode [21–24]. This is because carbon atoms on the surface of a CeO_2-based material (e.g., SDC, $Gd_xCe_{1-x}O_{2-\delta}$ (GDC)) can be trapped as oxidized carbon species rather than as solid carbon, which can mitigate and even kinetically prevent carbon deposition during CO_2 electrolysis, as shown in Fig. 4(b) [5]. Papaefthimiou et al. [21] suggested that CeO_2-based materials can participate in a carbon redox reaction via transformation between Ce(III) and Ce(IV), which substantially changes the CO_2 reduction pathways. By using *in situ* XPS, Yu et al. [22] identified obvious carbonate signals at the surface during the reduction process when the Ni–YSZ cathode is modified with CeO_2 or its derivatives. It is speculated that the carbon reduction reaction proceeds via the following mechanism:

$$CO_3^{2-} + 2Ce^{3+} \rightarrow CO + 2O^{2-} + 2Ce^{4+} \quad (5)$$

This reaction mechanism for carbon formation on Ni–YSZ and SDC surfaces explains the fact that SDC-based systems possess significantly enhanced coking resistance under SOEC operating conditions. This can be further confirmed by the intact interface between the SDC electrodes and electrolytes in cross-sectional SEM images, as shown in Fig. 4(c). The results clearly suggest that ceria or ceria-related oxides are promising and can be further developed as SOEC cathode candidates for catalyzing CO_2 electrochemical reduction.

Neagu et al. [23] and Yue et al. [24] found that the carbon deposition reaction rate on the Ni surface also strongly depends on the size of the metallic Ni particles in the composite cathode.

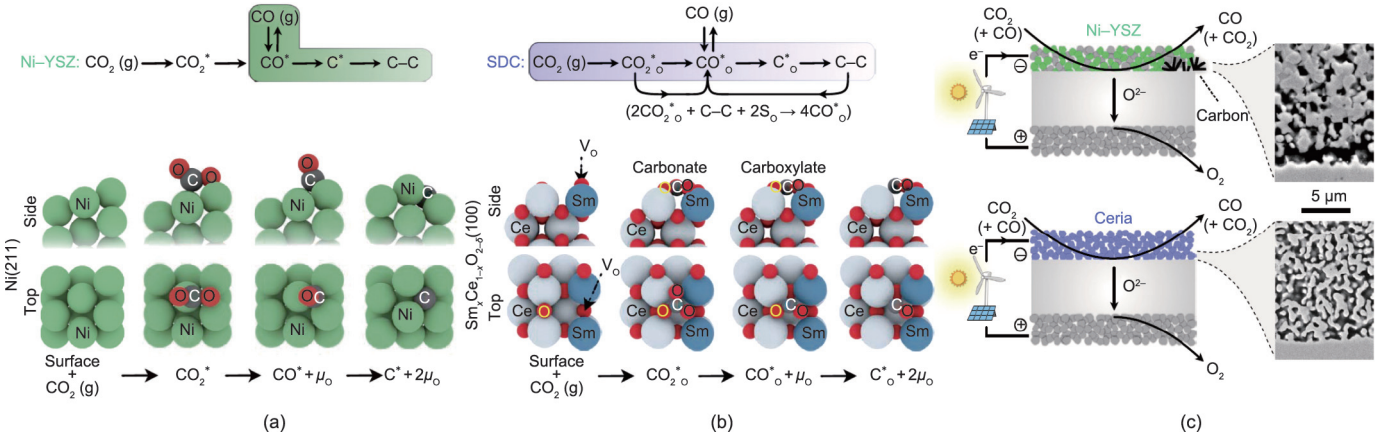

Fig. 4. Possible CO_2 reduction mechanism on the surface of (a) Ni–YSZ and (b) SDC under SOEC operating conditions; (c) cross-sectional SEM images of two types of cathode/electrolyte interfaces. Reproduced from Ref. [5] with permission.

Christensen et al. [25] and Chen et al. [26] explained that, in smaller Ni crystal grains, the saturation concentration of carbon is relatively higher; thus, the electrode possesses a higher tolerance to carbon. According to this principle, developing a new electrode preparation process and reducing the average particle size of the metallic Ni should be an effective strategy to improve the carbon resistance of composite cathodes. For example, by means of a [$Ni(acac)_2$] (acac stands for acetylacetone) precursor reduction, Han et al. [27] prepared Ni nanoparticles that were uniformly distributed on a silica surface, with an average particle size of only (5.2 ± 0.4) nm; after annealing these Ni nanoparticles at 800 °C under a methane (CH_4) atmosphere for about 170 h, there was still no detectable coke deposition on the surface. Liang et al. [28] developed a urea combustion *in situ* synthesis process to prepare a NiO–YSZ electrode material precursor (where the NiO possessed a particle size of about 11 nm); after H_2 reduction, fine and uniformly dispersed metallic Ni particles were generated on the YSZ matrix. However, the thermal and chemical stabilities of the metallic nanoparticles prepared by these methods still need to be further enhanced, and agglomeration of the metallic nanoparticles may become the main degeneration issue.

Another important series of materials that have been widely used as SOEC cathodes for CO_2 electrolysis are copper (Cu)-containing composites [29–32]. In particular, Cu–CeO_2–YSZ and its derivatives have been widely investigated as promising SOEC cathode materials, as these composites are inert for coke deposition and typically exhibit small decreases in the open circuit voltage (OCV) of the cell when exposed to a CO_2 or CO atmosphere [32,33]. For experimental verification, Cheng et al. [34] fabricated an adherent layer of porous Cu/$Gd_{0.1}Ce_{0.9}O_2$ (CGO) electrode on a YSZ electrolyte by sintering Cu/CGO paste onto a YSZ substrate. The Cu–CGO|YSZ|YSZ–LSM|LSM electrolysis cell based on this cathode was developed and exhibited no significant performance degradation during 2 h of CO_2 reduction at 750 °C with a 1:1 CO_2/CO feed. In another investigation, Su et al. [29] fabricated a Cu–SDC cathode supported on YSZ by means of an impregnating method and developed a Cu–SDC|YSZ|Cu–SDC symmetrical cell. The activation energy of CO_2 electrolysis reduction via this cell was measured to be as low as about 1.57 eV under a CO–CO_2 (50:50) or CO–CO_2 (67:33) atmosphere; impregnating more Cu produced more Cu–CeO_x interfaces and further lowered the activation energy. Liu et al. [33] developed a Cu/$Ce_{0.6}Mn_{0.3}Fe_{0.1}O_{2-\delta}$ electrode for a reversible solid oxide electrochemical cell with CO/CO_2 as the shuttle. In the electrolysis mode, the current density reached up to 2.2 A·cm^{-2} at 2.0 V and 800 °C. After 100 h of cycled operation between the SOEC and solid oxide fuel cell (SOFC) modes, the cell exhibited no degeneration, suggesting remarkable stability under CO/CO_2 conditions. These results demonstrate that Cu-containing composites possess unique advantages when used as cathode materials for high-temperature CO_2 electrolysis.

3.1.2. Perovskite-based cathodes

In recent years, it has been discovered that many perovskite-based oxides possess mixed ionic and electronic conductivity (MIEC) and considerable electrocatalytic activity, as well as high redox stability and resistance against coke deposition, suggesting that these materials can be used as superior SOEC cathode candidates [35–37]. Typical perovskite-based oxides include perovskite materials ($ABO_{3-\delta}$, where "A" is an alkaline earth or rare earth metal ion, and "B" is a transition metal ion), Ruddlesden–Popper materials ($A_2BO_{4+\delta}$), and double-perovskite materials ($AA'B_2O_{5+\delta}$), whose crystal structures are shown in Fig. 5 [2,38]. Many perovskite-based materials, including $La_{1-x}Sr_xCr_yMn_{1-y}O_{3-\delta}$ (LSCM), $La_{1-x}Sr_xFeO_{3-\delta}$ (LSF), and $La_{1-x}Sr_xTiO_{3-\delta}$ (LST), exhibit remarkable stability under a wide range of oxygen partial pressures, and there are abundant oxygen vacancies on their surface, which provide active sites for CO_2 chemical adsorption and subsequent carbon reduction [39–42].

LSCM, which has an acceptable ionic conductivity, remarkable electronic conductivity, and excellent durability under a CO/CO_2-containing atmosphere, is one of the most widely used perovskite-based SOEC cathode materials for CO_2 electrolysis or co-electrolysis [39,40,43]. Notably, YSZ or GDC are typically added into an LSCM cathode to enhance its ionic conductivity [40]. For example, using a vacuum infiltration method, Yue and Irvine [44] fabricated a Pd–GDC co-infiltrated LSCM cathode, which achieved a polarization resistance of only 0.24 Ω·cm^2 at 900 °C under a CO–CO_2 (30:70) atmosphere. Zhang et al. [45] developed an LSCM–GDC/YSZ composite cathode by co-sintering LSCM and GDC nanoparticles onto a porous YSZ scaffold. At 800 °C and a current density of 0.29 A·cm^{-1}, no particle aggregation or performance degeneration was observed during the 50 h test for the cathode. Recently, Ma et al. [46] synthesized an LSCM cathode using a glycine–nitrate process (GNP). An LSCM|YSZ|LSCF full cell based on this cathode showed a stable current density of 0.1 A·cm^{-2} at 800 °C under an H_2O–CO_2 (60:40) atmosphere at 1.5 V for 24 h, demonstrating remarkable durability toward CO_2 electrolysis and co-electrolysis.

LSF is another important cathode material candidate for high-temperature CO_2 electrolysis [39,40,47]. In previous studies, Yang et al. [48] developed an LSF|LSGM|LSCF (LSGM stands for $La_{0.9}Sr_{0.1}Ga_{0.95}Mg_{0.05}O_{3-\delta}$) single cell and achieved a current density of 0.76 A·cm^{-2} at 1.5 V and 800 °C under a pure CO_2 atmosphere. Zhou et al. [49] fabricated a palladium (Pd) single-

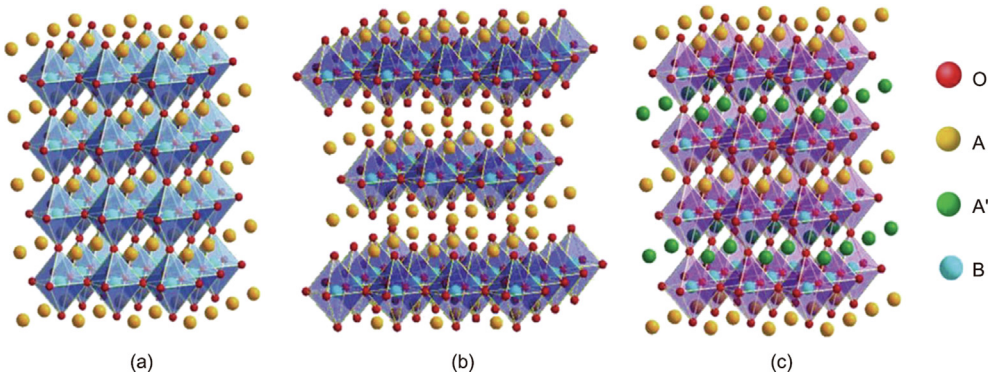

Fig. 5. Schematic diagram of the crystal structure of several perovskite-based oxides: (a) perovskite materials; (b) Ruddlesden–Popper materials; and (c) double-perovskite materials. Reproduced from Ref. [2] with permission.

site-anchored Pd–LSF–SDC cathode by means of ball milling and firing. The Pd–LSF–SDC|YSZ|LSM–YSZ single cell based on this cathode showed a highest average current density of 0.58 A·cm^{-2} at 1.6 V and 800 °C under a CO_2 atmosphere. These results demonstrate that LSF and its derivatives are promising candidates for cathode materials in high-temperature CO_2 electrolysis.

In addition, many other perovskite-based materials exhibit good performance when applied as SOEC cathodes for CO_2 electrolysis, including LST, (La,Sr)VO_3 (LSV), and $Sr_2Fe_{1.5}Mo_{0.5}O_{6-\delta}$ (SFM), which have been introduced and comprehensively summarized in previous review articles [39,40].

3.1.3. Cathodes with exsolved nanoparticles

Recently, many studies have demonstrated that, under an appropriate reducing atmosphere, the B-site transition metal ions in perovskite-based materials can be reduced and then exsolved on the surface, generating metallic nanoparticles or simple oxides in what is known as B-site cation exsolution (Fig. 6(a)) [41,50]. Typically, these metallic nanoparticles not only possess excellent electronic conductivity and electrochemical activity but also show special stability under high temperatures and reducing atmospheres; therefore, they can significantly improve the electrochemical performance of perovskite-based cathode materials [23,51]. For example, Lv et al. [52] fabricated a double-perovskite-structured $Sr_2Fe_{1.35}Mo_{0.45}Co_{0.2}O_{6-\delta}$ electrode and treated it under a 5% H_2/Ar atmosphere for 2 h at 800 °C to generate Co–Fe nanoparticles at the surface (Fig. 6(b)). They found that the polarization resistance of the electrode was reduced to about half of that before exsolution (Fig. 6(c)) [52]. Xie et al. [53] converted a $NbTi_{0.5}Ni_{0.5}O_4$ cathode into $Nb_{1.33}Ti_{0.67}O_4$/Ni nanoparticles by reducing it at 1200 °C under a 5% H_2/Ar atmosphere. After this reduction, the electronic conductivity of the cathode significantly increased from 0.001 to 92 S·cm^{-1}. The researchers further prepared a $Nb_{1.33}Ti_{0.67}O_4$ + Ni|YSZ|$La_{0.8}Sr_{0.2}MnO_{3+\delta}$–$Ce_{0.8}Sm_{0.2}O_{2-\delta}$ electrolysis cell based on the exsolved cathode, and the cell showed a good stability in a pure CO_2 atmosphere, with a Faraday efficiency of about 65%. No nanoparticle agglomeration or performance degradation was observed during five redox cycles [53]. In another investigation, Li et al. [54] treated an $(La_{0.2}Sr_{0.8})_{0.9}(Ti_{0.9}Mn_{0.1})_{0.9}Ni_{0.1}O_{3-\delta}$ cathode in 5% H_2/Ar to generate Ni nanoparticles on the electrode surface. They found that the exsolved Ni increased the Faraday efficiency of the electrolysis cell by about 20% during CO_2 electrolysis (Fig. 7(a)) [54]. Gan et al. [55] prepared an $(La_{0.3}Sr_{0.7})_{0.9}Ti_{0.95}Ni_{0.05}O_{3-\delta}$ cathode and reduced it in 5% H_2/Ar to produce Ni nanoparticles; the cathode achieved a Faraday efficiency of about 90% during CO_2 electrolysis, and the production of CO was increased significantly by four times (Fig. 7(b)). Gan et al. [56] synthesized an $La_{0.5}Ba_{0.5}Mn_{1-x}Co_xO_{3-\delta}$ cathode using the Pechini method and reduced it in 5% H_2/Ar for 2 h to generate exsolved metallic cobalt (Co). At 1.3 V and 850 °C, a single cell based on this cathode achieved a high current density of 0.88 A·cm^{-2} with 90% Faradaic efficiency. Yang et al. [57] fabricated an $(La_{0.2}Sr_{0.8})_{0.9}Ti_{0.5}Mn_{0.4}Cu_{0.1}O_{3-\delta}$ SOEC cathode with exsolved Cu nanoparticles. At 1.8 V and 800 °C, the single cell

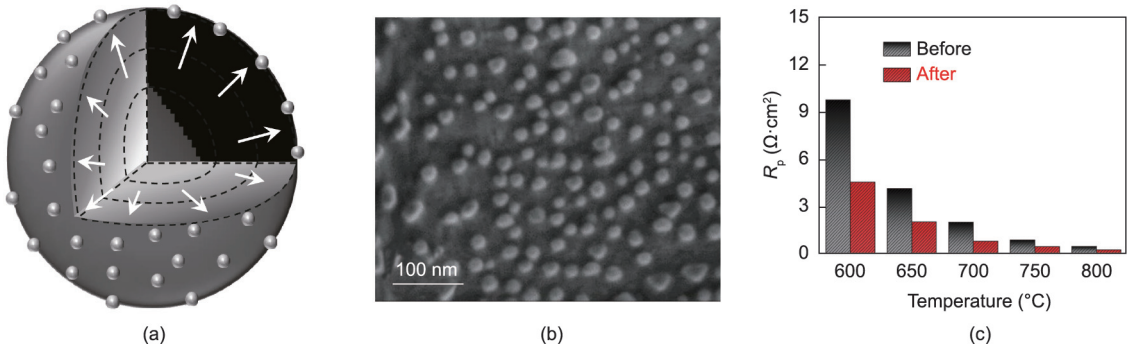

Fig. 6. (a) Illustration of B-site cation exsolution in perovskite cathode materials; (b) SEM image of $Sr_2Fe_{1.35}Mo_{0.45}Co_{0.2}O_{6-\delta}$ (SFMC) electrode materials after 2 h reduction and exsolution; (c) polarization resistance (R_p) of SFMC–GDC cells before and after 2 h reduction. (a) Reproduced from Ref. [50] with permission; (b, c) reproduced from Ref. [52] with permission.

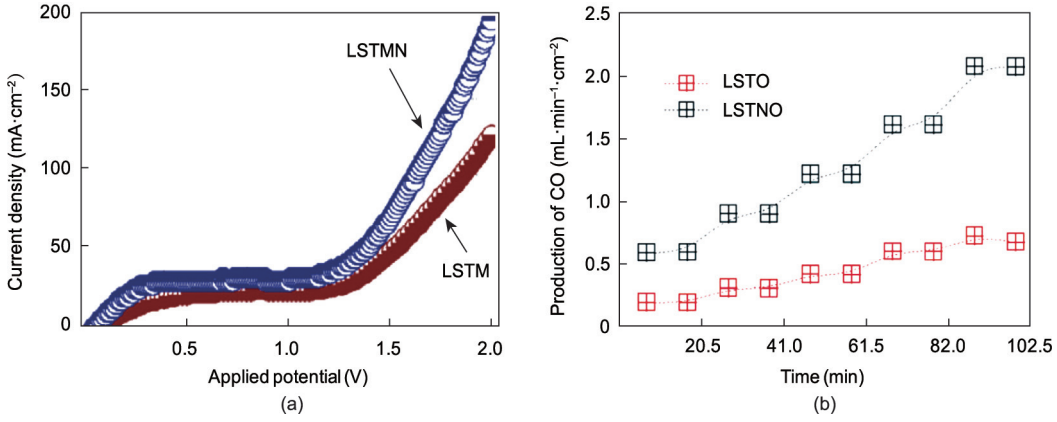

Fig. 7. (a) Electrochemical performance of an $(La_{0.2}Sr_{0.8})_{0.9}(Ti_{0.9}Mn_{0.1})_{0.9}Ni_{0.1}O_{3-\delta}$ (LSTMN) cathode before and after Ni exsolution (LSTM: $(La_{0.2}Sr_{0.8})(Ti_{0.9}Mn_{0.1})O_{3-\delta}$); (b) CO production for electrolyzers with $La_xSr_{1-x}TiO_{3+\delta}$ (LSTO) and $(La_{0.3}Sr_{0.7})_{0.9}Ti_{0.95}Ni_{0.05}O_{3-\delta}$ (LSTNO) cathodes. (a) Reproduced from Ref. [54] with permission; (b) reproduced from Ref. [55] with permission.

showed a high current density of 2.82 A·cm^{-2} under a pure CO_2 atmosphere, demonstrating extremely high electrochemical activity for CO_2 electrolysis.

Many investigations have demonstrated that the metallic nanoparticles generated by *in situ* exsolution on the surface of a perovskite cathode have considerable electronic conductivity and electrocatalytic activity, as well as possessing excellent resistance against carbon deposition during CO_2 electrolysis [38,41]. Using Raman spectroscopy, Liu et al. [42] investigated a $(Pr_{0.4}Sr_{0.6})_3(Fe_{0.85}Mo_{0.15})_2O_7$ electrode with exsolved Co–Fe nanoparticles and demonstrated that no graphite signal was detected on the electrode surface after 10 h of electrolysis operation at 850 °C under a CO_2–CO (70:30) atmosphere, while obvious graphite signals appeared on the surface of a conventional Ni–YSZ cathode under the same conditions (Fig. 8(a)). This finding suggests that exsolved Co–Fe nanoparticles possess much higher coke resistance than traditional SOEC cathodes. The coke resistance of Ni, Mn, Cr, Cu, and other exsolved metallic nanoparticles has also been confirmed in other SOEC cathode systems [58–61]. The performance of several cathodes with exsolved metallic nanoparticles during CO_2 electrolysis or co-electrolysis is listed in Table 1 [42,52,55,58–65]. More specifically, Neagu et al. [23] proposed that these exsolved metallic nanoparticles typically have an "anchoring" effect in their original position, and that their structural stability and chemical stability are much higher than those of composite material systems prepared by infiltration methods. Zhao et al. [66] pointed out that the metallic nanoparticles anchored on the cathode surface both promoted the electrochemical reduction kinetics of CO_2 and inhibited the carbon deposition process through rapid electron exchange, further accelerating the conversion from carbon on the surface into carbon-containing gas phase products (Fig. 8(b)). This finding explains the stability of these cathodes with exsolved nanoparticles during CO_2 electrolysis.

Although research on enhancing the electrochemical performance of perovskite electrodes by means of exsolved metallic nanoparticles has been widely confirmed in SOEC cathode systems, the mechanism or driving force of B-site exsolution remains unclear. Currently, it is generally accepted that the exsolution of B-site cations can be controlled by the distribution of the bulk/surface defects of the perovskite lattice and influenced by the external

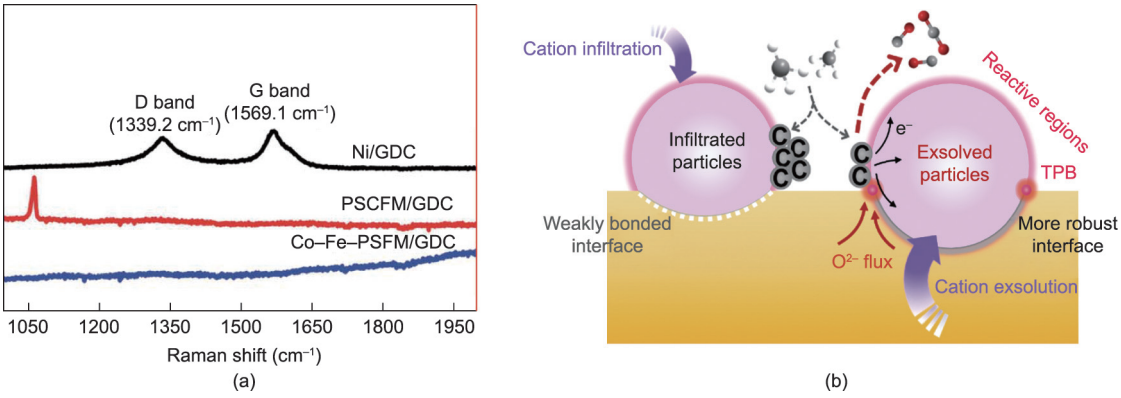

Fig. 8. (a) Raman spectra of Ni/GDC, $Pr_{0.4}Sr_{0.6}Co_{0.2}Fe_{0.7}Mo_{0.1}O_{3-\delta}$ (PSCFM)/GDC, and Co–Fe–$(Pr_{0.4}Sr_{0.6})_3(Fe_{0.85}Mo_{0.15})_2O_7$ (PSFM)/GDC cathodes after testing; (b) comparison of fuel electrodes fabricated by infiltration and exsolution (TPB: triple phase boundaries). (a) Reproduced from Ref. [42] with permission; (b) reproduced from Ref. [66] with permission.

Table 1
Performance of typical cathodes with exsolved metallic nanoparticles during CO_2 electrolysis.

Exsolved component	Composition of perovskite matrix	Performance during CO_2 electrolysis	Ref.
Fe	$Sr_2Fe_{1.5+x}Mo_{0.5}O_{6-\delta}$ (x = 0–0.1)	No carbon deposition after 100 h electrolysis at 850 °C under a CO_2/CH_4 atmosphere, 1.4 V electrolysis potential, and ~0.5 A·cm^{-2} current density	[63]
Co	$Pr_{0.5}Ba_{0.5}Mn_{1-y}Co_yO_x$	Stably electrolyzing under a CO/CO_2 atmosphere; current density reaches 0.85, 1.6, and 2.5 A·cm^{-2} at 800, 850, and 900 °C, respectively	[64]
Ni	$La_{0.43}Ca_{0.37}Ni_{0.06}Ti_{0.94}O_3$	No carbon deposition during 48 h electrolysis at 850 °C under a H_2O/CO_2 atmosphere at a current density of ~0.6 A·cm^{-2}; electrolysis potential only increased from 1.37 to 1.39 V during this process	[60]
	$(La_{0.3}Sr_{0.7})_{0.9}Ti_{0.95}Ni_{0.05}O_{3-\delta}$	Stable CO_2 electrolysis at 800 °C under a current density of ~0.3 A·cm^{-2} and a 2 V potential in an H_2O/CO_2 atmosphere with 90% Faraday efficiency	[55]
	$(La_{0.2}Sr_{0.8})_{0.95}Ti_{0.85}Mn_{0.1}Ni_{0.05}O_{3+\delta}$	Current density reaches 0.91 A·cm^{-2} when electrolyzing pure CO_2 at 850 °C and 2 V; no performance degradation during 10 redox cycles	[58]
Mn	$Nb_{1.33}(Ti_{0.8}Mn_{0.2})_{0.67}O_4$	Current density reaches ~1.6 A·cm^{-2} when electrolyzing at 800 °C, 1.6 V under a CO_2/CO/Ar atmosphere; stably operating for more than 100 h at 1.4 V with no degradation	[59]
Cr	$Nb_{1.33}(Ti_{0.8}Cr_{0.2})_{0.67}O_4$	Current density reaches ~1.6 A·cm^{-2} when electrolyzing at 800 °C, 1.6 V under a CO_2/CO/Ar atmosphere; stably operating for more than 100 h at 1.4 V with no degradation	[59]
Ni–Cu alloy	$NbTi_{0.5}(Ni_xCu_{1-x})_{0.5}O_4$	CO output reaches 0.1629 mL·min^{-1}·cm^{-2} when running at 800 °C, 1.4 V potential in a pure CO_2 atmosphere	[61]
Co–Fe alloy	$(Pr_{0.4}Sr_{0.6})_3(Fe_{0.85}Mo_{0.15})_2O_7$	No carbon deposits detected on the electrode surface after 10 h continuous electrolysis operation at 850 °C under a CO_2–CO (70:30) atmosphere	[42]
	$Sr_2Fe_{1.35}Mo_{0.45}Co_{0.2}O_{6-\delta}$	Stable CO_2 electrolysis at 800 °C with a current density of 1.2 A·cm^{-2} at 1.6 V, no performance degradation occurred in 12 oxidation–reduction cycles	[52]
Fe–Ni alloy	$La_{0.6}Sr_{0.4}Fe_{0.8}Ni_{0.2}O_{3-\delta}$	Current density reaches 1.78 A·cm^{-2} when electrolyzing CO_2/CO at 850 °C and 1.6 V; stably operating for more than 100 h at a current density of ~1.37 A·cm^{-2}	[65]
Fe–MnO	$(Pr,Ba)Mn_{1-x}Fe_xO_{3-\delta}$	Stable electrolysis of pure CO_2 at 850 °C with a current density of 638 mA·cm^{-2} at 1.6 V	[62]

oxidation/reduction conditions [38,41,67]. When the perovskite lattice is reduced, oxygen vacancies are typically generated on the surface rather than within the bulk, while these surface defect sites tend to attract B-site transition metal cations within the bulk due to the charge effect. The existence of surface defects also decreases the barrier to the nucleation of metallic nanoparticles, thus accelerating the reduction and nucleation of B-site cations [23,41]. Such effects can continuously drive the B-site cations inside the crystal lattice to migrate to the outermost surface and can cause the exsolved metallic nanoparticles to continue to grow until a balance is reached [23,67]. In the future, with the development of *in situ* characterization technology and theoretical simulation methods, we expect to obtain a clearer understanding of the exsolution mechanism and kinetic process of B-site transition metal cations. This will allow us to obtain a better understanding of the precise control of cation exsolution behaviors, which will be useful for guiding the design of perovskite-based SOEC cathode materials with high electrochemical activity and high stability.

3.2. Anode materials

Regardless of water electrolysis or CO_2 electrolysis, the oxygen evolution reaction (OER; $2O^{2-} \rightarrow O_2 + 4e^-$) occurring at the oxygen electrode is one of the most critical steps in electrochemical conversion [68]. The evolution of oxygen molecules is a four-electron process that possesses a high reaction energy barrier and relatively slow kinetics, and it often acts as the origin of the overpotential [69]. In order to improve the efficiency of the electrolysis reaction and reduce the polarization resistance and overpotential, anode materials are usually expected to possess the following properties: ① considerable electronic conductivity; ② considerable ionic conductivity; ③ abundant surface oxygen vacancies and a relatively low formation energy of oxygen vacancy; and ④ a porous morphology, which provides numerous channels for the diffusion and release of the generated O_2 during electrolysis.

The most widely used SOEC anode materials are perovskite-based oxides, such as LSM, $La_{1-x}Sr_xCo_{1-y}Fe_yO_{3-\delta}$ (LSFC), $La_{1-x}Sr_xCoO_{3-\delta}$ (LSC), and LSF, although these materials also have their own shortcomings in practice [2,70,71]. For example, LSM, which was commonly used as an SOEC anode material in the early years of this field, possesses high chemical and structural stability, as well as considerable electronic conductivity. However, its oxygen vacancy formation energy is relatively high and its ionic conductivity is low, resulting in insufficient electrocatalytic activity [38,72]. In comparison, LSC, which has considerable MIEC and electrocatalytic activity, possesses insufficient stability at high temperatures, and surface side reactions such as strontium (Sr) segregation are prone to occur; thus, the performance degradation issue is a bottleneck during long-term operation [38,72–75]. Therefore, achieving a balance between electrochemical activity and stability for anode materials is a key problem that needs to be solved in this field.

Studies have shown that decorating perovskite anode materials with precious metals or their compounds can simultaneously improve the electrocatalytic activity and the operational stability. For example, Li et al. [76] used a surface infiltration method to decorate an $La_{0.5}Ba_{0.25}Sr_{0.25}Co_{0.8}Fe_{0.2}O_{3-\delta}$ (LBSCF) porous anode with RuO_2 nanoparticles (the anode loaded by RuO_2 is referred to as LBSCF–Ru) and found that rapid material transfer and charge transfer could occur in the RuO_2/perovskite interfacial region, contributing to a significant drop in polarization impedance. The electrolysis cell Ni–YSZ|YSZ|LBSCF–Ru based on this anode exhibited no detectable degradation during a pure CO_2 electrolysis process at 850 °C and 1.6 V with a high current density of 2.26 A·cm^{-2} for 90 h, thus demonstrating excellent durability for CO_2 electrolysis. Song et al. [77] modified a YSZ anode with extrinsic gold (Au) and further fabricated a Ni–YSZ|YSZ|Au–YSZ electrolysis cell, which achieved a steady pure-CO_2 electrolysis during 100 h of operation at 800 °C with no degradation. Such modification methods contribute to a step change in the development of confined electrodes with superior stability and activity for SOEC applications. However, the question of how to reduce the amount of precious metals in such electrodes in order to control the cost of anode manufacturing is still a problem that must be further considered in practical applications.

Aside from enhancing the electrocatalytic activity and chemical stability of electrode materials, it is crucial to improve the structural robustness and mechanical stability of the electrode. The OER occurring at the SOEC anode is a process in which the number of gas molecules increases. The commonly used sponge-like anodes generally contain a huge number of tortuous pores or closed pores. As a result, the gas diffusion property is usually unsatisfied, resulting in insufficient capability for the release of the generated oxygen. In particular, while operating at an elevated current density, increased oxygen production may lead to the formation of localized high-oxygen-pressure sites inside the anode, which causes delamination of the anode/electrolyte interface. This results in a sharp increase in the polarization resistance, endangering the long-term operational stability of the electrolysis cell [70,78]. To address this issue, optimizing the gas diffusion in the anode is crucial in order to enhance the stability against degradation under a high current density.

To reduce the gas diffusion resistance of an SOEC anode, a novel skeleton structure has been designed and remarkable results have been achieved. For example, Chen et al. [79] fabricated a microchannel-structured $Gd_{0.1}Ce_{0.9}O_{2-\delta}$ (GDC) framework by means of a freezing-casting method and subsequently obtained an $Sm_{0.5}Sr_{0.5}CoO_3$–$Gd_{0.1}Ce_{0.9}O_{2-\delta}$ (SSC–GDC) porous anode via an infiltration–sintering method. The SSC–GDC|GDC|Ni–GDC cell based on this electrode was further demonstrated to have an extremely low polarization resistance of only 0.05 Ω·cm^2 at 600 °C, indicating excellent potential for electrolysis applications. Wu et al. [80] further optimized a frozen preparation technique for the oxygen electrode skeleton and successfully prepared a novel honeycomb-structured LSC–YSZ microchannel anode with regular morphology and extremely high pore density. The polarization resistance of this honeycomb-structured anode was only 0.0094 Ω·cm^2 at 800 °C, and the corresponding symmetrical cell could operate at a large current density of 2 A·cm^{-2} with no detectable performance degradation during 6 h of operation. Based on these results, Li et al. [81] prepared an LSF–GDC|GDC–YSZ|Ni–GDC electrolysis cell with a microchannel anode and applied it in pure CO_2 electrolysis. The cell exhibited good stability under a large current density of 2.5 A·cm^{-2} at 800 °C, and no performance degradation was observed within 124 h of operation (Fig. 9) [81]. These fundamental research results provide guidance for the rational design of high-performance anodes for SOECs, as well as for the large-scale commercial application of SOECs in the field of CO_2 electrolysis.

3.3. Electrolyte materials

The electrolyte of an SOEC is positioned between the cathode and anode. Although it does not directly participate in the electrochemical reaction, the electrolyte still plays a vital role in determining the overall performance of the electrolysis cell [82,83]. In general, the function of the electrolyte is to conduct ionic charge carriers (e.g., oxygen ions), as well as blocking electronic conduction and preventing gas leakage. The following characteristics are thus typically required for the electrolyte materials of an SOEC: ① a relatively high ionic conductivity and almost no electronic conductivity under the operating conditions, to prevent short circuiting inside the electrolysis cell; ② a thermal expansion

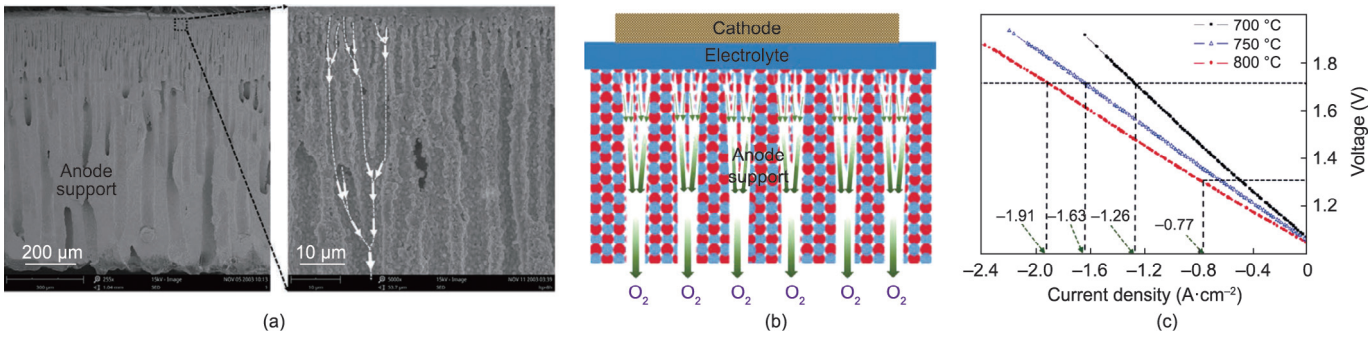

Fig. 9. (a) SEM images of the channeled electrode; (b) oxygen release path in the bulk of the electrode; (c) electrolysis polarization curve of the electrolyzer. Reproduced from Ref. [81] with permission.

coefficient that is basically matched with those of both the hydrogen electrode and the oxygen electrode materials; ③ low reactivity with the hydrogen electrode and oxygen electrode materials; ④ structural durability and chemical stability under strong oxidizing and reducing conditions; and ⑤ a dense morphology to prevent the interdiffusion and leakage of gases on the anode side and cathode side [2].

Commonly used electrolyte materials for oxygen-ion-conducting SOECs (known as O-SOECs) include doped zirconium-based oxides (e.g., YSZ), cerium-based oxides (e.g., SDC), and several perovskite-structured oxides (e.g., LSGM) [2]. The relationship between conductivity, temperature, and thickness is shown in Fig. 10 [83]. It can be seen that increasing the operating temperature and reducing the thickness of the electrolyte are effective methods to enhance the electrical conductivity.

YSZ is one of the most mature electrolyte materials for high-temperature SOECs due to its considerable ionic conductivity, excellent durability, and acceptable price [84,85]. Nevertheless, several challenges still exist, which have hindered its further industrial application [2,66]. For example, many researchers have suggested that there are typically numerous grain boundaries in a dense YSZ electrolyte layer, which possess an ionic conductivity 1–2 orders of magnitude lower than that of the YSZ grains [84,86]. In addition, it has been widely observed that, when operating at high temperatures, YSZ is likely to react with many anode components (e.g., LSM or LSC), forming a $La_2Zr_2O_7$ or $SrZrO_3$ secondary insulating phase and thus leading to degradation of the electrolyte conductivity [2,82,87]. To address these problems, cerium-based oxides are usually added to enhance the performance of YSZ. For example, Shen et al. [88] added TiO_2 and SDC into a YSZ electrolyte and found that the ionic conductivity of YSZ significantly increased from 0.09 to 0.123 $S{\cdot}cm^{-1}$ at 1000 °C, probably because the additives reduced the sintering temperature and increased the grain size. In another study, Kim et al. [89] fabricated a 7 μm-thick $Ce_{0.43}Zr_{0.43}Gd_{0.1}Y_{0.04}O_{2-\delta}$ (CZGY) contact layer and further developed an LSCF|GDC|CZGY|YSZ|Ni–YSZ electrolysis cell. During the 100 h steam electrolysis, no significant degeneration was observed; the authors attributed the excellent durability to the enhanced interface stability and the small amount of Sr segregation of the LSCF anode.

In addition to conventional YSZ, the development of novel high-performance electrolyte materials is of great significance for improving the overall performance of SOECs. Recently, certain perovskite-based oxides have been developed as promising electrolyte material candidates for SOECs due to their remarkable ionic conductivity and excellent stability at elevated temperatures. For example, LSGM, which is one of the most commonly used perovskite-based electrolyte materials, possesses significantly higher ionic conductivity than YSZ [82,90]. As reported by Elangovan et al. [91], a 300 mm-thick LSGM electrolyte with an

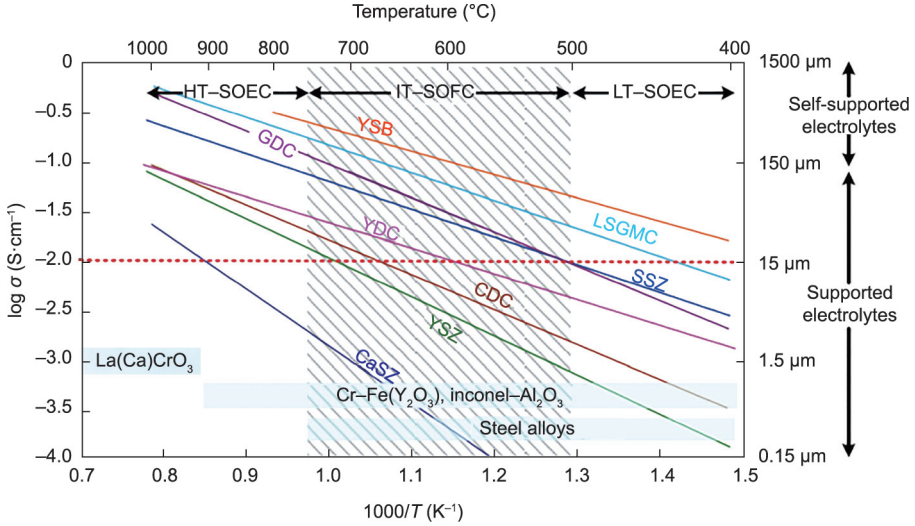

Fig. 10. Commonly used electrolyte materials for O-SOECs and their conductivity (HT: high temperature; IT: intermediate temperature; LT: low temperature; YSB: $(Bi_2O_3)_{0.75}(Y_2O_3)_{0.25}$; LSGMC: $La_xSr_{1-x}Ga_yMg_{1-y-z}Co_zO_3$; SSZ: $(ZrO_2)_{0.8}(Sc_2O_3)_{0.2}$; YDC: $Ce_{0.8}Y_{0.2}O_{1.96}$; CDC: $Ce_{0.9}Ca_{0.1}O_{1.8}$; CaSZ: $Zr_{0.85}Ca_{0.15}O_{1.85}$). Reproduced from Ref. [83] with permission.

LSC anode and a Ni–MgO–ceria cathode exhibited an area-specific resistance of only 0.6 Ω·cm^2 at 800 °C; moreover, the area-specific resistance of an LSGM-supported ten-cell stack was only 1 Ω·cm^2 at 800 °C. Despite these advantages, LSGM electrolytes tend to react with metallic Ni to generate an inactive $LaNiO_3$ phase, so modifications on anodes are still required to avoid such side reactions [82]. Fop et al. [92] developed a novel hexagonal perovskite derivative, $Ba_3MoNbO_{8.5}$, which showed excellent stability and exhibited a relatively high oxide ionic conductivity of 2.2×10^{-3} S·cm^{-1} at 600 °C. Hopefully, the development and utilization of these novel electrolytes can significantly enhance the electrochemical performance of SOECs, in what could be a new direction for the future development of SOEC components.

Another research direction for optimizing SOEC electrolytes is to reduce its thickness, as a thin and stable electrolyte layer can significantly reduce the ohmic loss of electrolysis and greatly improve the electrolysis performance [11]. In the future, the development and application of new preparation technologies such as molecular beam epitaxy (MBE), atomic layer deposition (ALD), and pulsed-laser deposition (PLD) [85,93] may bring revolutionary changes in this field, greatly accelerating the pace of the large-scale industrialization of CO_2 high-temperature electrolysis technology.

4. SOEC-coupled chemical carbon-reduction techniques

It can be concluded from the aforementioned discussion that the components involved in SOECs typically possess the characteristics of affordability, structural stability, and performance stability under elevated temperature and a carbon-containing atmosphere. Such properties will not only contribute to the large-scale promotion of SOEC technology in the future but also make the device suitable for relatively complex chemical synthesis systems. By integrating the SOEC high-temperature electrolysis process with several chemical synthesis processes, various fuels or chemical raw materials can be produced, which is a promising route for taking advantage of SOECs.

4.1. SOEC modular design and scale-up

In order to meet the different scale demands for industrial application, modular designs of SOEC systems are necessary. Through modular design, single cells with uniform size can be arranged together to form an SOEC stack, and several stacks can be further assembled into an SOEC module (Fig. 11) [94]. In general, an increase in the number of modules can lead to enhanced surface area, resulting in elevated production capacity. Therefore, a modular design can enlarge the size of SOECs and promote their industrial application. It also increases the flexibility and reliability of SOEC systems.

Here, it should be noted that SOEC systems operating in complex environments should include many necessary components in addition to the stack itself. For example, a heat management system can recover the heat contained in outlet products and therefore improve the overall electrolysis efficiency; a purification system can adjust the composition of the inlet gas and remove the impurities that may attenuate the stack; and an automatic control system can remotely control the SOEC module [2,4]. These system accessories have also undergone tremendous recent development; however, instability and unreliability still exist, and the unreliability of these system components has actually become the most common reason for system breakdown [4]. Thus, in future, the development and optimization of these system accessories are still necessary in order to further improve the operational stability and reliability of SOEC stacks and modules.

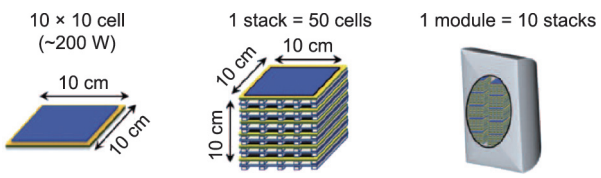

Fig. 11. Illustration of arranging single cells of a uniform size together to form stacks and modules. Reproduced from Ref. [94] with permission.

4.2. SOEC application scenarios in the chemical industry

In application scenarios involving SOECs coupled with processes in the chemical industry, one of the most well-known technical paths is the production of CO/H_2 synthesis gas by co-electrolyzing the high-temperature waste gas generated in chemical processes, and then converting the synthesis gas into methane, ethylene, liquid hydrocarbons, alcohols, and other chemical raw materials through the Fischer–Tropsch synthesis reaction [1,2,14]. This route can use the waste gas and waste heat generated by the chemical process effectively; it can also convert CO_2 into liquid carbon-containing products, which is of great significance for achieving the goals of a carbon peak and carbon neutrality. For experimental verification, Chen et al. [14] designed an SOEC-coupled Fischer–Tropsch synthesis device consisting of a tubular SOEC high-temperature electrolysis unit (an LSM–YSZ|YSZ|Ni–YSZ tubular electrolysis cell, operating at ~800 °C) and a Fischer–Tropsch synthesis unit (operating at ~250 °C), as illustrated in Fig. 12. When the intake air was about 15 mL·min^{-1} CO_2/H_2 (CO_2:H_2 = 1:6) and the relative humidity was 20%, the methane yield at the outlet was 0.84 mL·min^{-1}, and the CO_2 conversion rate reached 64%. Furthermore, Luo et al. [95] prepared an LSGM-based tubular SOEC that achieved one-step CH_4 production, with a high CO_2-to-CH_4 conversion ratio of 98.7%. More recently, Lee et al. [96] developed a six-cell flat-tubular Ni–YSZ|YSZ–GDC|LSCF–GDC SOEC bundle with a total active area of 240 cm^2, which achieved durable co-electrolysis for a continuous 500 h at a H_2O/CO_2 ratio of 2 at 800 °C. These results preliminarily demonstrate the feasibility of this technology path at the laboratory scale.

In recent years, due to continuous development and optimization, CO_2 high-temperature electrolysis technology based on SOECs is ready for industrial scale-up, and its scaling up has been proceeding rapidly. In 2017, Küngas et al. [97] from Haldor Topsøe A/S reported the world's first commercial CO_2 electrolysis system (eCOs), which can deliver more than 10 normal cubic meters (Nm^3) CO per hour at 99.995% purity. Two years later, they further provided the test data of their stacks with improved components: Under the conditions of 750 °C and –70 A, a single SOEC stack with 2.2 Nm^3·h^{-1} CO production capability can operate for more than 5000 h with no detectable degeneration [98]. Based on these developments, Haldor Topsøe A/S was prepared to develop several commercial plants that would be able to produce 96 Nm^3·h^{-1} CO at > 99.95% purity in the next two years [97,98]. In 2019, Posdziech et al. [99] from Sunfire GmbH developed a co-electrolysis demonstration system that integrated three stacks to produce syngas (Fig. 13). The system could be fed by different H_2O/CO_2 mixtures, and the maximum production rate of syngas was 4 Nm^3·h^{-1} with 10 kW inlet power. In 2020, Dannesboe et al. [100] from both Aarhus University and Haldor Topsøe A/S reported that they had successfully combined an SOEC system with the downstream synthesis process for upgrading biogas to pipeline quality biomethane in a pilot plant yielding 10 Nm^3·h^{-1}. This system had been running continuously for more than 2000 h, the power consumption of the SOEC stack was about 3.07 kW·h·Nm^{-3} H_2, and the power utilization efficiency reached approximately 80%

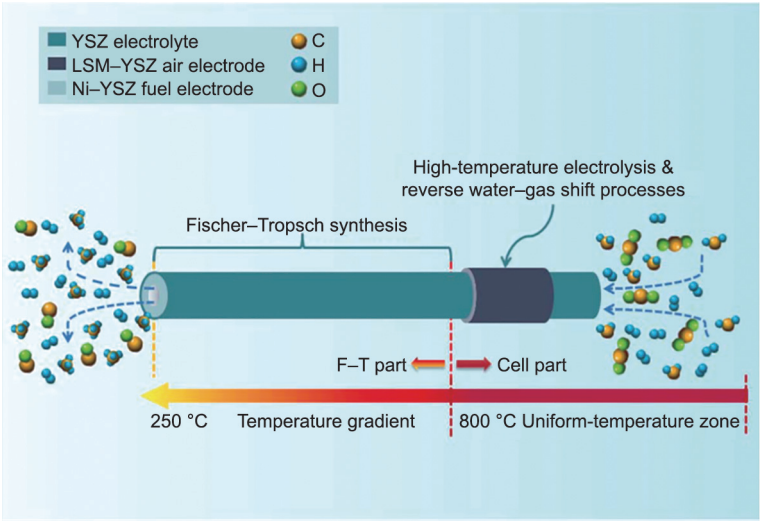

Fig. 12. Schematic diagram of direct methane synthesis from CO_2–H_2O co-electrolysis in a unit combining an SOEC and a Fischer–Tropsch (F–T) reactor. Reproduced from Ref. [14] with permission.

Fig. 13. A co-electrolysis system demonstration developed by Sunfire GmbH. Reproduced from Ref. [99] with permission.

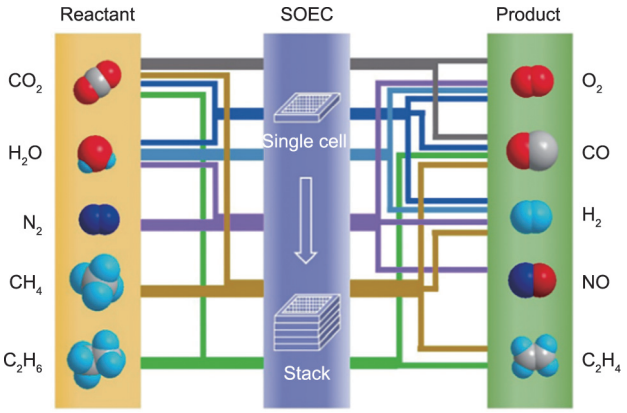

Fig. 14. Schematic diagram of various chemical processes based on SOEC reactors. Reproduced from Ref. [1] with permission.

[101]. Recently, the New Energy and Industrial Technology Development Organization in Japan declared that a total of about 4.5 billion JPY will be invested in 2020–2024 to develop the integrated production technology of CO_2 electrolysis and the Fischer–Tropsch synthesis to produce liquid synthetic fuels (gasoline, diesel, aviation fuel, etc.) [4].

In addition to producing hydrocarbon fuels, researchers have developed SOEC technology for the precise synthesis of specific small molecules, such as the directional synthesis of C_2H_4 and NO, as shown in Fig. 14 [1]. These small molecules can be further subjected to catalytic oxidation, polymerization, or other reactions to obtain a series of high-value-added products such as fertilizers, synthetic resins, and synthetic rubbers.

It is accepted that the production of small molecules by means of SOECs has unique advantages in terms of overall efficiency, because SOECs can be operated at a relatively high current density (especially for CO_2 electrolysis), which represents high output [4]. In addition, the integration of SOECs with several chemical production processes (e.g., synthesis of methane, methanol, and ammonia) has many advantages from the perspective of energy utilization (Fig. 15) [4]. It should be noted that all the above processes involve exothermic reactions; thus, the heat released can be utilized to produce the steam needed as feedstock for the SOEC, which further maximizes the use of energy and has a substantial synergistic effect. In addition, for coupling with ammonia synthesis, the distinctive capability of the SOEC to function as an oxygen separation membrane is taken advantage of; the use of heat in lieu of power can be harnessed to eliminate the need for an expensive air separation unit to provide nitrogen (Fig. 15(c)). These synthetic methods indicate the possibility of overturning the traditional fabrication route of chemical products mainly derived from petroleum. In the future, with the further development of renewable energy power generation technology and the price reduction of renewable electricity, such oil-free SOEC-coupling chemical preparation and synthesis processes are expected to become novel technical routes for the chemical industry.

4.3. Challenges and future research directions

Although significant progress has been made in this field, several technological achievements must be made in order to realize the large-scale application of high-temperature CO_2 electrolysis. These include: ① the development of highly active and stable cell components; ② large-scale CO_2 collecting and purification technology; ③ highly efficient heat management systems for high-

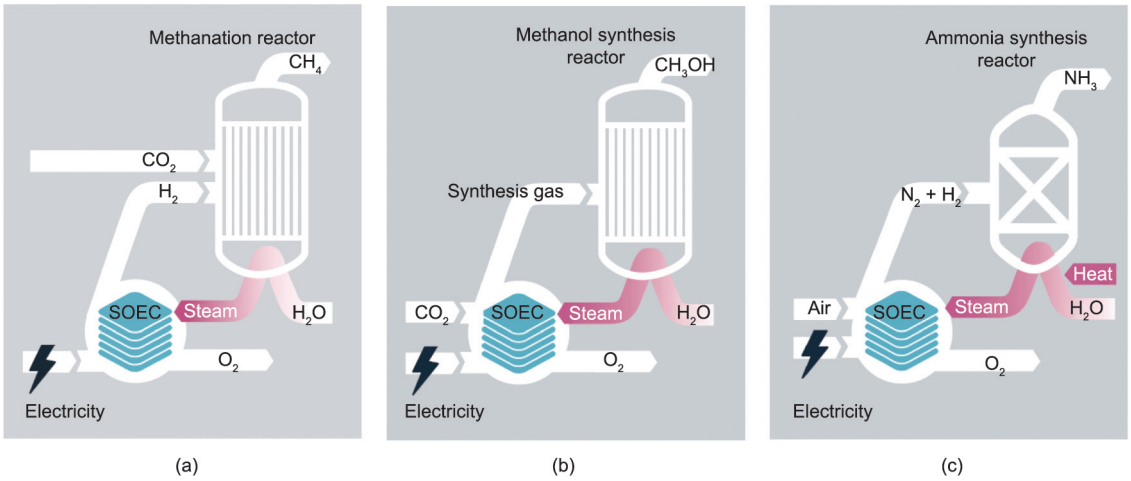

Fig. 15. Schematic diagram of an SOEC coupling chemical synthesis and carbon reduction process: (a) methane synthesis; (b) methanol synthesis; and (c) ammonia synthesis. Reproduced from Ref. [4] with permission.

temperature SOEC stacks; and ④ separation and purification technology for obtaining single-component outlet gas [2,102]. Thus far, several solutions have been proposed for enhancing the performance of SOEC-based CO_2 conversion systems [103–107]. For example, given that the feed gases of CO_2 produced from natural gas or coal gasification may contain impurities such as H_2S, a series of sulfur-resistant materials have been applied as SOEC cathodes, and various inlet gas pretreatment systems have been developed to mitigate electrode poisoning [2,105]. In addition, to improve the thermal efficiency of the conversion systems, the heat released during an exothermic chemical synthesis process has been designed to be utilized in the form of latent or sensible heat [103]. Moreover, to obtain concentrated CO_2 from air or industrial plants, alkaline chemical absorbents have been proposed as intermediates for large-scale CO_2 storage and release [107]. In the future, with the development and application of these related technologies, the reliability and operational stability of high-temperature CO_2 electrolysis devices can be further enhanced.

Nevertheless, several economic issues are still presented by SOEC technology, including: ① high operation and maintenance costs due to the degradation issues of the cell components; ② high production costs due to the high electricity consumption; and ③ high construction costs due to a lack of standardized manufacturing techniques and the limited scale of currently existing SOEC plants [1,2]. To address these challenges, we suggest the following areas as future research directions:

(1) Exploring cheap cell component materials with high electrochemical properties and considerable stability, thus mitigating material degradation and extending the lifespan of the stack. Moreover, fundamental research focusing on the degeneration mechanism of SOEC components in *in situ* environments is necessary for the rational design of more durable cell materials and stacks.

(2) Developing single cells with novel structures (e.g., honeycomb-structured microchannel electrodes) to further facilitate the kinetics of the elementary reaction steps (including gas adsorption, electron transfer, ion diffusion, etc.) of high-temperature electrolysis, as well as promoting the systematization and scaling-up of single cells into stacks and modules, while ensuring air tightness and operating stability.

(3) Exploring the coupling mode of high-temperature electrolysis and renewable energy, which mainly involves developing SOEC stacks and modules that can operate continuously and stably under the intermittent electricity input from renewable energy sources.

Such improvements are expected to significantly reduce the operating costs of SOEC and broaden its application scenarios, as well as further promote SOEC-coupled chemical industry carbon neutralization solutions.

5. Conclusion and outlook

CO_2 high-temperature electrolysis technology based on SOECs holds great importance for achieving China's goals of carbon emission reduction, peak carbon emission, and carbon neutralization. By consuming electricity, SOECs can directly convert CO_2 (or CO_2/H_2O) into CO (or hydrocarbon fuels), thereby realizing the recycling utilization of CO_2. Great progress has been made in CO_2 high-temperature electrolysis technology at the laboratory and pilot stages, although the large-scale industrial application of this technology still needs further development. The main challenges include how to improve the operating efficiency and stability at a high temperature and high current density, and how to promote the systematization and scaling-up of single cells into stacks and modules while ensuring long-term durability. To address these challenges, it is essential to explore low-cost cell component materials with excellent electrochemical properties and considerable stability, develop cells and stacks with novel structures, and explore the coupling mode of high-temperature electrolysis and renewable energy. In the future, fundamental research on high-temperature electrochemistry requires further effort, and the application of advanced *in situ* characterization methods and simulation analysis methods should be accelerated to provide guidance for the rational design of materials suitable for high-performance CO_2 electrolysis. Furthermore, key accessories for high-temperature CO_2 electrolysis systems should be developed, including power supplies, gas purification systems, gas circulation systems, and temperature-control systems. Meanwhile, comprehensive simulations and experimental studies should be accelerated to verify the economic and technical feasibility of SOEC-coupled chemical carbon reduction technology, thereby laying down a theoretical and experimental basis for the establishment of a large-scale CO_2 recycling utilization industrial chain.

Compliance with ethics guidelines

Yifeng Li, Longgui Zhang, Bo Yu, Jianxin Zhu, and Changjiang Wu declare that they have no conflict of interest or financial conflicts to disclose.

References

[1] Zheng Y, Chen Z, Zhang J. Solid oxide electrolysis of H_2O and CO_2 to produce hydrogen and low-carbon fuels. Electrochem Energy Rev 2021;4(3):508–17.
[2] Zheng Y, Wang J, Yu B, Zhang W, Chen J, Qiao J, et al. A review of high temperature co-electrolysis of H_2O and CO_2 to produce sustainable fuels using solid oxide electrolysis cells (SOECs): advanced materials and technology. Chem Soc Rev 2017;46(5):1427–63.
[3] Gao S, Lin Y, Jiao X, Sun Y, Luo Q, Zhang W, et al. Partially oxidized atomic cobalt layers for carbon dioxide electroreduction to liquid fuel. Nature 2016;529(7584):68–71.
[4] Hauch A, Küngas R, Blennow P, Hansen AB, Hansen JB, Mathiesen BV, et al. Recent advances in solid oxide cell technology for electrolysis. Science 2020;370(6513):eaba6118.
[5] Skafte TL, Guan Z, Machala ML, Gopal CB, Monti M, Martinez L, et al. Selective high-temperature CO_2 electrolysis enabled by oxidized carbon intermediates. Nat Energy 2019;4(10):846–55.
[6] Elliott D. A balancing act for renewables. Nat Energ 2016;1(1):15003.
[7] Ebbesen SD, Jensen SH, Hauch A, Mogensen MB. High temperature electrolysis in alkaline cells, solid proton conducting cells, and solid oxide cells. Chem Rev 2014;114(21):10697–734.
[8] Adler SB. Factors governing oxygen reduction in solid oxide fuel cell cathodes. Chem Rev 2004;104(10):4791–844.
[9] Jensen SH, Larsen PH, Mogensen M. Hydrogen and synthetic fuel production from renewable energy sources. Int J Hydrogen Energy 2007;32(15):3253–7.
[10] Alenazey F, Alyousef Y, Almisned O, Almutairi G, Ghouse M, Montinaro D, et al. Production of synthesis gas (H_2 and CO) by high-temperature co-electrolysis of H_2O and CO_2. Int J Hydrogen Energy 2015;40(32):10274–80.
[11] Zhang W, Yu B. Development status and prospects of hydrogen production by high temperature solid oxide electrolysis. J Electrochem 2020;26(2):212–29.
[12] Zheng Y, Zhang W, Li Y, Chen J, Yu B, Wang J, et al. Energy related CO_2 conversion and utilization: advanced materials/nanomaterials, reaction mechanisms and technologies. Nano Energy 2017;40:512–39.
[13] Jiang Y, Chen F, Xia C. A review on cathode processes and materials for electro-reduction of carbon dioxide in solid oxide electrolysis cells. J Power Sources 2021;493:229713.
[14] Chen L, Chen F, Xia C. Direct synthesis of methane from CO_2–H_2O co-electrolysis in tubular solid oxide electrolysis cells. Energy Environ Sci 2014;7(12):4018–22.
[15] Hartvigsen J, Elangovan S, Elwell J, Larsen D. Oxygen production from Mars atmosphere carbon dioxide using solid oxide electrolysis. ECS Trans 2017;78(1):2953–63.
[16] Hansen JB. Solid oxide electrolysis—a key enabling technology for sustainable energy scenarios. Faraday Discuss 2015;182:9–48.
[17] Ebbesen SD, Høgh J, Nielsen KA, Nielsen JU, Mogensen M. Durable SOC stacks for production of hydrogen and synthesis gas by high temperature electrolysis. Int J Hydrogen Energy 2011;36(13):7363–73.
[18] Nguyen VN, Fang Q, Packbier U, Blum L. Long-term tests of a Jülich planar short stack with reversible solid oxide cells in both fuel cell and electrolysis modes. Int J Hydrogen Energy 2013;38(11):4281–90.
[19] Hauch A, Ebbesen SD, Jensen SH, Mogensen M. Solid oxide electrolysis cells: microstructure and degradation of the Ni/yttria-stabilized zirconia electrode. J Electrochem Soc 2008;155(11):B1184–93.
[20] Argyle MD, Bartholomew CH. Heterogeneous catalyst deactivation and regeneration: a review. Catalysts 2015;5(1):145–269.
[21] Papaefthimiou V, Shishkin M, Niakolas DK, Athanasiou M, Law YT, Arrigo R, et al. On the active surface state of nickel–ceria solid oxide fuel cell anodes during methane electrooxidation. Adv Energy Mater 2013;3(6):762–9.
[22] Yu Y, Mao B, Geller A, Chang R, Gaskell K, Liu Z, et al. CO_2 activation and carbonate intermediates: an operando AP-XPS study of CO_2 electrolysis reactions on solid oxide electrochemical cells. Phys Chem Chem Phys 2014;16(23):11633–9.
[23] Neagu D, Oh TS, Miller DN, Ménard H, Bukhari SM, Gamble SR, et al. Nano-socketed nickel particles with enhanced coking resistance grown *in situ* by redox exsolution. Nat Commun 2015;6(1):8120.
[24] Yue W, Li Y, Zheng Y, Wu T, Zhao C, Zhao J, et al. Enhancing coking resistance of Ni/YSZ electrodes: *in situ* characterization, mechanism research, and surface engineering. Nano Energy 2019;62:64–78.
[25] Christensen KO, Chen D, Lødeng R, Holmen A. Effect of supports and Ni crystal size on carbon formation and sintering during steam methane reforming. Appl Catal A Gen 2006;314(1):9–22.
[26] Chen D, Christensen KO, Ochoa-Fernández E, Yu Z, Tøtdal B, Latorre N, et al. Synthesis of carbon nanofibers: effects of Ni crystal size during methane decomposition. J Catal 2005;229(1):82–96.
[27] Han JW, Kim C, Park JS, Lee H. Highly coke-resistant Ni nanoparticle catalysts with minimal sintering in dry reforming of methane. ChemSusChem 2014;7(2):451–6.
[28] Liang M, Yu B, Wen M, Chen J, Xu J, Zhai Y. Preparation of NiO–YSZ composite powder by a combustion method and its application for cathode of SOEC. Int J Hydrogen Energy 2010;35(7):2852–7.
[29] Su T, Li Y, Xue S, Xu Z, Zheng M, Xia C. Kinetics of CO_2 electrolysis on composite electrodes consisting of Cu and samaria-doped ceria. J Mater Chem A 2019;7(4):1598–606.
[30] Kumari N, Haider MA, Tiwari PK, Basu S. Carbon dioxide reduction on the composite of copper and praseodymium-doped ceria electrode in a solid oxide electrolysis cells. Ionics 2019;25(7):3165–77.
[31] Kumari N, Tiwari PK, Haider MA, Basu S. Electrochemical performance of infiltrated Cu–GDC and Cu–PDC cathode for CO_2 electrolysis in a solid oxide cell. ECS Trans 2017;78(1):3329–37.
[32] Wang W, Vohs JM, Gorte RJ. Hydrogen production via CH_4 and CO assisted steam electrolysis. Top Catal 2007;46(3–4):380–5.
[33] Liu L, Wang Y, Zhou X, Yang Y, Ma C, Li Y, et al. Cu/$Ce_{0.6}Mn_{0.3}Fe_{0.1}O_{2-\delta}$ membrane fuel electrode fabricated by infiltration method for solid oxide electrochemical cells. Electrochim Acta 2017;235:365–73.
[34] Cheng CY, Kelsall GH, Kleiminger L. Reduction of CO_2 to CO at Cu–ceria-gadolinia (CGO) cathode in solid oxide electrolyser. J Appl Electrochem 2013;43(11):1131–44.
[35] Zhao B, Zhang L, Zhen D, Yoo S, Ding Y, Chen D, et al. A tailored double perovskite nanofiber catalyst enables ultrafast oxygen evolution. Nat Commun 2017;8(1):14586.
[36] Zhou Y, Guan X, Zhou H, Ramadoss K, Adam S, Liu H, et al. Strongly correlated perovskite fuel cells. Nature 2016;534(7606):231–4.
[37] Graves C, Ebbesen SD, Jensen SH, Simonsen SB, Mogensen MB. Eliminating degradation in solid oxide electrochemical cells by reversible operation. Nat Mater 2015;14(2):239–44.
[38] Li Y, Zhang W, Zheng Y, Chen J, Yu B, Chen Y, et al. Controlling cation segregation in perovskite-based electrodes for high electro-catalytic activity and durability. Chem Soc Rev 2017;46(20):6345–78.
[39] Ma Z, Zhou J, Li Y, Liu C, Pu J, Chen X. Developments in CO_2 electrolysis of solid oxide electrolysis cell with different cathodes. Fuel Cells 2020;20(6):650–60.
[40] Zhang X, Song Y, Wang G, Bao X. Co-electrolysis of CO_2 and H_2O in high-temperature solid oxide electrolysis cells: recent advance in cathodes. J Energy Chem 2017;26(5):839–53.
[41] Irvine JTS, Neagu D, Verbraeken MC, Chatzichristodoulou C, Graves C, Mogensen MB. Evolution of the electrochemical interface in high-temperature fuel cells and electrolysers. Nat Energy 2016;1(1):15014.
[42] Liu S, Liu Q, Luo JL. CO_2-to-CO conversion on layered perovskite with *in situ* exsolved Co–Fe alloy nanoparticles: an active and stable cathode for solid oxide electrolysis cells. J Mater Chem A 2016;4(44):17521–8.
[43] Yue X, Irvine JTS. (La, Sr)(Cr, Mn)O_3/GDC cathode for high temperature steam electrolysis and steam–carbon dioxide co-electrolysis. Solid State Ion 2012;225:131–5.
[44] Yue X, Irvine JTS. Modification of LSCM–GDC cathodes to enhance performance for high temperature CO_2 electrolysis using solid oxide electrolysis cells (SOECs). J Mater Chem A 2017;5(15):7081–90.
[45] Zhang X, Song Y, Guan F, Zhou Y, Lv H, Liu Q, et al. $(La_{0.75}Sr_{0.25})_{0.95}(Cr_{0.5}Mn_{0.5})$-$O_{3-\delta}$–$Ce_{0.8}Gd_{0.2}O_{1.9}$ scaffolded composite cathode for high temperature CO_2 electroreduction in solid oxide electrolysis cell. J Power Sources 2018;400:104–13.
[46] Ma Z, Li Y, Zheng Y, Li W, Chen X, Sun X, et al. $La_{0.75}Sr_{0.25}Cr_{0.5}Mn_{0.5}O_{3-\delta}$ as cathode for electrolysis and co-electrolysis of CO_2 and H_2O in solid oxide electrolysis cell. Ceram Int 2021;47(16):23350–61.
[47] Pidburtnyi M, Zanca B, Coppex C, Jimenez-Villegas S, Thangadurai V. A review on perovskite-type $LaFeO_3$ based electrodes for CO_2 reduction in solid oxide electrolysis cells: current understanding of structure–functional property relationships. Chem Mater 2021;33(12):4249–68.
[48] Yang Y, Li Y, Jiang Y, Zheng M, Hong T, Wu X, et al. The electrochemical performance and CO_2 reduction mechanism on strontium doped lanthanum ferrite fuel electrode in solid oxide electrolysis cell. Electrochim Acta 2018;284:159–67.
[49] Zhou Y, Lin L, Song Y, Zhang X, Lv H, Liu Q, et al. Pd single site-anchored perovskite cathode for CO_2 electrolysis in solid oxide electrolysis cells. Nano Energy 2020;71:104598.
[50] Myung J, Neagu D, Miller DN, Irvine JTS. Switching on electrocatalytic activity in solid oxide cells. Nature 2016;537(7621):528–31.
[51] Kwon O, Sengodan S, Kim K, Kim G, Jeong HY, Shin J, et al. Exsolution trends and co-segregation aspects of self-grown catalyst nanoparticles in perovskites. Nat Commun 2017;8(1):15967.
[52] Lv H, Lin L, Zhang X, Song Y, Matsumoto H, Zeng C, et al. *In situ* investigation of reversible exsolution/dissolution of CoFe alloy nanoparticles in a Co-doped $Sr_2Fe_{1.5}Mo_{0.5}O_{6-\delta}$ cathode for CO_2 electrolysis. Adv Mater 2020;32(6):1906193.
[53] Xie K, Zhang J, Xu S, Ding B, Wu G, Xie T, et al. Composite cathode based on redox-reversible $NbTi_{0.5}Ni_{0.5}O_4$ decorated with *in situ* grown Ni particles for direct carbon dioxide electrolysis. Fuel Cells 2014;14(6):1036–45.
[54] Li Y, Xie K, Chen S, Li H, Zhang Y, Wu Y. Efficient carbon dioxide electrolysis based on perovskite cathode enhanced with nickel nanocatalyst. Electrochim Acta 2015;153:325–33.
[55] Gan L, Ye L, Tao S, Xie K. Titanate cathodes with enhanced electrical properties achieved via growing surface Ni particles toward efficient carbon dioxide electrolysis. Phys Chem Chem Phys 2016;18(4):3137–43.
[56] Gan J, Hou N, Yao T, Fan L, Gan T, Huang Z, et al. A high performing perovskite cathode with *in situ* exsolved Co nanoparticles for H_2O and CO_2 solid oxide electrolysis cell. Catal Today 2021;364:89–96.
[57] Yang X, Sun W, Ma M, Xu C, Ren R, Qiao J, et al. Achieving highly efficient carbon dioxide electrolysis by *in situ* construction of the heterostructure. ACS Appl Mater Interfaces 2021;13(17):20060–9.

[58] Ye L, Zhang M, Huang P, Guo G, Hong M, Li C, et al. Enhancing CO_2 electrolysis through synergistic control of non-stoichiometry and doping to tune cathode surface structures. Nat Commun 2017;8(1):14785.
[59] Wang W, Gan L, Lemmon JP, Chen F, Irvine JTS, Xie K. Enhanced carbon dioxide electrolysis at redox manipulated interfaces. Nat Commun 2019;10(1):1550.
[60] Kyriakou V, Neagu D, Papaioannou EI, Metcalfe IS, van de Sanden MCM, Tsampas MN. Co-electrolysis of H_2O and CO_2 on exsolved Ni nanoparticles for efficient syngas generation at controllable H_2/CO ratios. Appl Catal B 2019;258:117950.
[61] Wei H, Xie K, Zhang J, Zhang Y, Wang Y, Qin Y, et al. *In situ* growth of Ni_xCu_{1-x} alloy nanocatalysts on redox-reversible rutile $(Nb,Ti)O_4$ towards high-temperature carbon dioxide electrolysis. Sci Rep 2015;4(1):5156.
[62] Zhu J, Zhang W, Li Y, Yue W, Geng G, Yu B. Enhancing CO_2 catalytic activation and direct electroreduction on *in-situ* exsolved Fe/MnO_x nanoparticles from $(Pr, Ba)_2Mn_{2-y}Fe_yO_{5+\delta}$ layered perovskites for SOEC cathodes. Appl Catal B 2020;268:118389.
[63] Zhu C, Hou S, Hu X, Lu J, Chen F, Xie K. Electrochemical conversion of methane to ethylene in a solid oxide electrolyzer. Nat Commun 2019;10(1):1173.
[64] Sun YF, Zhang YQ, Chen J, Li JH, Zhu YT, Zeng YM, et al. New opportunity for *in situ* exsolution of metallic nanoparticles on perovskite parent. Nano Lett 2016;16(8):5303–9.
[65] Liu S, Liu Q, Luo JL. Highly stable and efficient catalyst with *in situ* exsolved Fe–Ni alloy nanospheres socketed on an oxygen deficient perovskite for direct CO_2 electrolysis. ACS Catal 2016;6(9):6219–28.
[66] Zhao C, Li Y, Zhang W, Zheng Y, Lou X, Yu B, et al. Heterointerface engineering for enhancing the electrochemical performance of solid oxide cells. Energy Environ Sci 2020;13(1):53–85.
[67] Neagu D, Tsekouras G, Miller DN, Ménard H, Irvine JTS. *In situ* growth of nanoparticles through control of non-stoichiometry. Nat Chem 2013;5(11):916–23.
[68] Zheng Y, Li Y, Wu T, Zhang W, Zhu J, Li Z, et al. Oxygen reduction kinetic enhancements of intermediate-temperature SOFC cathodes with novel $Nd_{0.5}Sr_{0.5}CoO_{3-\delta}/Nd_{0.8}Sr_{1.2}CoO_{4\pm\delta}$ heterointerfaces. Nano Energy 2018;51:711–20.
[69] Suntivich J, May KJ, Gasteiger HA, Goodenough JB, Shao-Horn Y. A perovskite oxide optimized for oxygen evolution catalysis from molecular orbital principles. Science 2011;334(6061):1383–5.
[70] Chen K, Jiang SP. Review—materials degradation of solid oxide electrolysis cells. J Electrochem Soc 2016;163(11):F3070–83.
[71] Jiang SP. Challenges in the development of reversible solid oxide cell technologies: a mini review. Asia-Pac J Chem Eng 2016;11(3):386–91.
[72] Koo B, Kim K, Kim JK, Kwon H, Han JW, Jung WC. Sr segregation in perovskite oxides: why it happens and how it exists. Joule 2018;2(8):1476–99.
[73] Tsvetkov N, Lu Q, Sun L, Crumlin EJ, Yildiz B. Improved chemical and electrochemical stability of perovskite oxides with less reducible cations at the surface. Nat Mater 2016;15(9):1010–6.
[74] Rupp GM, Opitz AK, Nenning A, Limbeck A, Fleig J. Real-time impedance monitoring of oxygen reduction during surface modification of thin film cathodes. Nat Mater 2017;16(6):640–5.
[75] Li Y, Zhang W, Wu T, Zheng Y, Chen J, Yu B, et al. Segregation induced self-assembly of highly active perovskite for rapid oxygen reduction reaction. Adv Energy Mater 2018;8(29):1801893.
[76] Li M, Hua B, Chen J, Zhong Y, Luo JL. Charge transfer dynamics in RuO_2/perovskite nanohybrid for enhanced electrocatalysis in solid oxide electrolyzers. Nano Energy 2019;57:186–94.
[77] Song Y, Zhou S, Dong Q, Li Y, Zhang X, Ta N, et al. Oxygen evolution reaction over the Au/YSZ interface at high temperature. Angew Chem Int Ed 2019;58(14):4617–21.
[78] Virkar AV. Mechanism of oxygen electrode delamination in solid oxide electrolyzer cells. Int J Hydrogen Energy 2010;35(18):9527–43.
[79] Chen Y, Lin Y, Zhang Y, Wang S, Su D, Yang Z, et al. Low temperature solid oxide fuel cells with hierarchically porous cathode nano-network. Nano Energy 2014;8:25–33.
[80] Wu T, Zhang W, Li Y, Zheng Y, Yu B, Chen J, et al. Micro-/nanohoneycomb solid oxide electrolysis cell anodes with ultralarge current tolerance. Adv Energy Mater 2018;8(33):1802203.
[81] Li T, Wang T, Wei T, Hu X, Ye Z, Wang Z, et al. Robust anode-supported cells with fast oxygen release channels for efficient and stable CO_2 electrolysis at ultrahigh current densities. Small 2021;17(6):2007211.
[82] Hauch A, Ebbesen SD, Jensen SH, Mogensen M. Highly efficient high temperature electrolysis. J Mater Chem 2008;18(20):2331–40.
[83] Brett DJL, Atkinson A, Brandon NP, Skinner SJ. Intermediate temperature solid oxide fuel cells. Chem Soc Rev 2008;37(8):1568–78.
[84] Chen IW, Kim SW, Li J, Kang SJL, Huang F. Ionomigration of neutral phases in ionic conductors. Adv Energy Mater 2012;2(11):1383–9.
[85] Jiang J, Hertz JL. On the variability of reported ionic conductivity in nanoscale YSZ thin films. J Electroceram 2014;32(1):37–46.
[86] Lenser C, Menzler NH. Impedance characterization of supported oxygen ion conducting electrolytes. Solid State Ion 2019;334:70–81.
[87] Yang K, Shen JH, Yang KY, Hung IM, Fung KZ, Wang MC. Formation of $La_2Zr_2O_7$ or $SrZrO_3$ on cathode-supported solid oxide fuel cells. J Power Sources 2006;159(1):63–7.
[88] Shen CT, Lee KR, Hsieh YP, Lee SW, Chang JK, Jang SC, et al. Effects of TiO_2 and SDC addition on the properties of YSZ electrolyte. Int J Hydrogen Energy 2019;44(56):29426–31.
[89] Kim SJ, Kim KJ, Choi GM. Effect of $Ce_{0.43}Zr_{0.43}Gd_{0.1}Y_{0.04}O_{2-\delta}$ contact layer on stability of interface between GDC interlayer and YSZ electrolyte in solid oxide electrolysis cell. J Power Sources 2015;284:617–22.
[90] Gao R, Jain ACP, Pandya S, Dong Y, Yuan Y, Zhou H, et al. Designing optimal perovskite structure for high ionic conduction. Adv Mater 2020;32(1):1905178.
[91] Elangovan S, Hartvigsen JJ, Frost LJ. Intermediate temperature reversible fuel cells. Int J Appl Ceram Technol 2007;4(2):109–18.
[92] Fop S, Skakle JMS, McLaughlin AC, Connor PA, Irvine JTS, Smith RI, et al. Oxide ion conductivity in the hexagonal perovskite derivative $Ba_3MoNbO_{8.5}$. J Am Chem Soc 2016;138(51):16764–9.
[93] Choi S, Kucharczyk CJ, Liang Y, Zhang X, Takeuchi I, Ji HI, et al. Exceptional power density and stability at intermediate temperatures in protonic ceramic fuel cells. Nat Energy 2018;3(3):202–10.
[94] Wachsman ED, Lee KT. Lowering the temperature of solid oxide fuel cells. Science 2011;334(6058):935–9.
[95] Luo Y, Shi Y, Li W, Cai N. Synchronous enhancement of H_2O/CO_2 co-electrolysis and methanation for efficient one-step power-to-methane. Energy Convers Manage 2018;165:127–36.
[96] Lee DY, Mehran MT, Kim J, Kim S, Lee SB, Song RH, et al. Scaling up syngas production with controllable H_2/CO ratio in a highly efficient, compact, and durable solid oxide coelectrolysis cell unit-bundle. Appl Energy 2020;257:114036.
[97] Küngas R, Blennow P, Heiredal-Clausen T, Nørby TH, Rass-Hansen J, Primdahl S, et al. eCOs—a commercial CO_2 electrolysis system developed by Haldor Topsøe. ECS Trans 2017;78(1):2879–84.
[98] Küngas R, Blennow P, Heiredal-Clausen T, Nørby TH, Rass-Hansen J, Hansen JB, et al. Progress in SOEC development activities at Haldor Topsøe. ECS Trans 2019;91(1):215–23.
[99] Posdziech O, Geißler T, Schwarze K, Blumentritt R. System development and demonstration of large-scale high-temperature electrolysis. ECS Trans 2019;91(1):2537–46.
[100] Dannesboe C, Hansen JB, Johannsen I. Catalytic methanation of CO_2 in biogas: experimental results from a reactor at full scale. React Chem Eng 2020;5(1):183–9.
[101] Hansen JB, Fock F, Lindboe HH. Biogas upgrading: by steam electrolysis or co-electrolysis of biogas and steam. ECS Trans 2013;57(1):3089–97.
[102] Song Y, Zhang X, Xie K, Wang G, Bao X. High-temperature CO_2 electrolysis in solid oxide electrolysis cells: developments, challenges, and prospects. Adv Mater 2019;31(50):1902033.
[103] Andika R, Nandiyanto ABD, Putra ZA, Bilad MR, Kim Y, Yun CM, et al. Co-electrolysis for power-to-methanol applications. Renew Sustain Energy Rev 2018;95:227–41.
[104] Sapountzi FM, Gracia JM, Weststrate CJKJ, Fredriksson HOA, Niemantsverdriet JWH. Electrocatalysts for the generation of hydrogen, oxygen and synthesis gas. Prog Energy Combust Sci 2017;58:1–35.
[105] Wang Y, Liu T, Lei L, Chen F. High temperature solid oxide H_2O/CO_2 co-electrolysis for syngas production. Fuel Process Technol 2017;161:248–58.
[106] Giglio E, Lanzini A, Santarelli M, Leone P. Synthetic natural gas via integrated high-temperature electrolysis and methanation: part I—energy performance. J Energy Storage 2015;1:22–37.
[107] Graves C, Ebbesen SD, Mogensen M, Lackner KS. Sustainable hydrocarbon fuels by recycling CO_2 and H_2O with renewable or nuclear energy. Renew Sustain Energy Rev 2011;15(1):1–23.